



Features of Metabolite Changes in Disease Evolution in Cholecystolithiasis

Kun Zhang^{1,2} · Yongzheng Wang³ · Xiaoxuan Cui¹ · Wei Wang³ · Yuliang Li³

Received: 26 July 2023 / Accepted: 28 September 2023 / Published online: 9 November 2023
© The Author(s) 2023

Abstract

Background Cholecystolithiasis is defined as a disease caused by complex and changeable factors. Advanced age, female sex, and a hypercaloric diet rich in carbohydrates and poor in fiber, together with obesity and genetic factors, are the main factors that may predispose people to choledocholithiasis. However, serum biomarkers for the rapid diagnosis of choledocholithiasis remain unclear.

Aims This study was designed to explore the pathogenesis of cholecystolithiasis and identify the possible metabolic and lipidomic biomarkers for the diagnosis of the disease.

Methods Using UHPLC-MS/MS and GC-MS, we detected the serum of 28 cholecystolithiasis patients and 19 controls. Statistical analysis of multiple variables included Principal Component Analysis (PCA). Visualization of differential metabolites was performed using volcano plots. The screened differential metabolites were further analyzed using clustering heatmaps. The quality of the model was assessed using random forests.

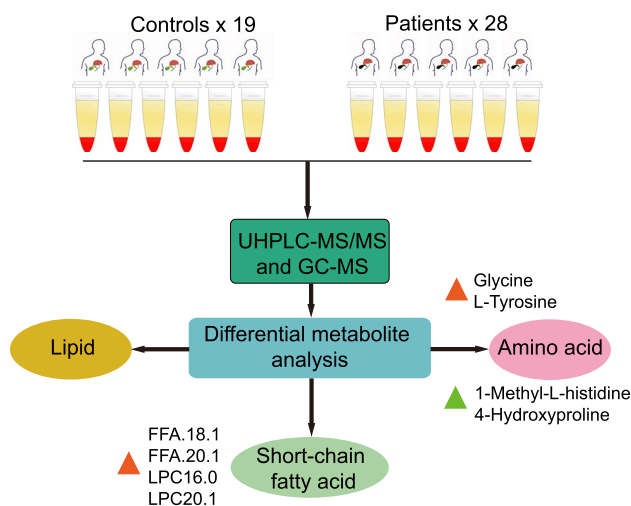
Results In this study, dramatically altered lipid homeostasis was detected in cholecystolithiasis group. In addition, the levels of short-chain fatty acids and amino acids were noticeably changed in patients with cholecystolithiasis. They detected higher levels of FFA.18.1, FFA.20.1, LPC16.0, and LPC20.1, but lower levels of 1-Methyl-L-histidine and 4-Hydroxyproline. In addition, glycine and L-Tyrosine were higher in choledocholithiasis group. Analyses of metabolic serum in affected patients have the potential to develop an integrated metabolite-based biomarker model that can facilitate the early diagnosis and treatment of the disease.

Conclusion Our results highlight the value of integrating lipid, amino acid, and short-chain fatty acid to explore the pathophysiology of cholecystolithiasis disease, and consequently, improve clinical decision-making.

Graphical Abstract

Using UHPLC-MS/MS and GC-MS, the serum of 28 cholecystolithiasis patients and 19 controls were analyzed. Through differential metabolite analysis, we found that the cholecystolithiasis group was detected with dramatically altered lipid homeostasis compared with healthy controls. In addition, the levels of short-chain fatty acids and amino acids were noticeably changed in patients with cholecystolithiasis. They detected higher levels of FFA.18.1, FFA.20.1, LPC16.0, and LPC20.1, but lower levels of 1-Methyl-L-histidine and 4-Hydroxyproline. Moreover, glycine and L-Tyrosine were higher in

choledocholithiasis group. The results not only identify new targets for the clinical diagnosis and treatment of cholecystolithiasis but may also provide valuable insights for the research of the disease.



Keywords Cholecystolithiasis · Lipid · Amino acid · Short-chain fatty acid · Free fatty acid (FFA) · Lysophosphatidylcholine (LPC)

Introduction

Cholecystolithiasis in the gallbladder is a common disease. Cholecystolithiasis has a mean prevalence rate of 10% according to epidemiological studies [1]. The incidence rate increases with changes in dietary patterns. In addition, the population is seriously aging [2–6]. In an increasingly obese population, cholecystolithiasis becomes a significant and growing health problem [7] and the cholecystolithiasis prevalence is rising [8]. However, cholecystolithiasis is an acute or chronic infection of the gallbladder [9]. Transcutaneous ultrasonography is the gold standard for diagnosing cholecystolithiasis [10]. Common bile duct (CBD) stones are primarily classified into two types: cholesterol and pigment, according to the stone major composition [11].

The main reason of cholesterol stones is that metabolic abnormalities in the hepatobiliary system is the primary reason. The formation of cholesterol stones is a complex process that involves interactions between genetic and environmental factors [12]. The liver is principally responsible for the regulation of biliary lipid and cholesterol concentration, which is a key determinant of the formation of cholesterol stones [13–15]. The primary pathophysiological defect in cholesterol cholecystolithiasis is the conflict between hypersecretion of hepatic cholesterol into bile and hyposecretion of bile salts and/or phospholipids [14]. Recently, homocystein has been reported to be another factor affecting such

a hepatic metabolism and is to be a clinical parameter for lithogenic risk, which is still to be established [16].

Bilirubin is one of the major constituents of bile that play an important role in formation process. However, in the center of cholesterol gallstones, bilirubin is also found, where it exists as calcium salts of unconjugated bilirubin (UCB) [17, 18]. The earliest mechanism suggestion for formation of pigment gallstone came from Maki [19]. Based on the reported results, it showed the key factor of bilirubin free radical that initiates and promotes pigment gallstone to formate [20]. Cholecystolithiasis is also strongly associated with gallbladder, pancreatic, and colorectal cancer occurrence. So, if treatment is not done promptly, cancer can be developed. In addition, higher plasma levels of branched chain amino acids (BCAAs) observed in patients with cholecystolithiasis may be partly responsible for metabolic complications observed in these patients [21].

To date, little is known about metabolomic and lipidomic perturbations in patients with cholecystolithiasis. Therefore, further research and screening the pathogenesis of cholecystolithiasis are urgent to identify biomarkers to diagnose cholecystolithiasis. In this study, we examined serum samples from 28 patients with cholecystolithiasis and 19 healthy controls. We adopted a global and systematic integrated analysis of changes in the lipidome profile in cholecystolithiasis. Collectively, the data show that the lipidome profile in the serum of cholecystolithiasis patients is markedly perturbed. Such

perturbations are noticeable at the preclinical phase before the disease progresses to definitive free fatty acid (FFA) and lysophosphatidylcholine (LPC), and these changes also reflect FFA and LPC activity and treatment outcome. The present study compared the lipidomic signature of cholecystolithiasis patients with that of healthy subjects.

Materials and Methods

Clinical Samples

A cross-sectional study was performed to compare metabolome profiling between patients with cholecystolithiasis (stone group) and healthy controls (control group). For the stone group, 28 consecutive patients scheduled for laparoscopic cholecystectomy with symptomatic cholecystolithiasis in the Hepatopancreatobiliary Surgery Department, Second Hospital of Shandong University were included. Ultrasonography of the gallbladder revealed cholecystolithiasis. Recurrence of biliary colic was observed in the patients, but those with cholecystolithiasis or acute cholecystitis were excluded. Meanwhile, 19 healthy volunteers receiving physical examination at the Health Center of the same hospital were recruited as the control group. Informed written consent was obtained from all participants. The study was approved by the hospital's Institutional Review Board and performed in accordance with the Declaration of Helsinki. Blood samples were collected and basic physiological indicators were taken from all participants. Serum samples were also prepared from the blood samples and stored immediately at -80°C for further analysis.

Metabolite Extraction for GC–MS

A total of 0.1 mL of each sample were transferred into a 1.5-mL Eppendorf (EP) tube. The sample was added with 0.05-mL 50% H_2SO_4 and 0.2 mL of extraction solution, which was methyl tert-butyl ether based (HPLC-grade, Shanghai Anpel Scientific Instrument Co., China) using 25-mg/L 2-Methylvaleric acid (≥ 99.5 , Augsburg, Germany) as an internal standard. The sample was vortexed for 10 s, oscillated for 10 min, and then sonicated for 10 min in ice water. Afterward, the sample was centrifuged for 15 min at 10,000 rpm at 4°C and placed at -20°C for 30 min. The obtained supernatant was transferred into an auto-sampler vial for GC–MS analysis.

GC–MS Analysis

The GC–MS analysis was performed using a SHIMADZU GC2030-QP2020 NX GC–MS system (Shimadzu, Tokyo, Japan) equipped with an HP-FFAP capillary column

($30\text{ m} \times 250\ \mu\text{m} \times 0.25\ \mu\text{m}$, J&W Scientific, Folsom, CA, USA). Helium was used as the carrier gas, with the front inlet purge flow set at 3 mL/min, and gas flow rate at 1 mL/min. The temperature conditions were programmed as follows: 80°C for 1 min, increased to 200°C at a rate of $10^{\circ}\text{C}/\text{min}$ and held for 5 min, and increased to 240°C at a rate of $40^{\circ}\text{C}/\text{min}$ and held for 1 min. The temperatures for injection, transfer line, quad, and ion source were 240°C , 240°C , 150°C , and 200°C , respectively. The electron energy was 70 eV.

Metabolite Extraction for UHPLC-MS/MS

A 15- μL aliquot of each individual sample was precisely transferred to an EP tube. A 15- μL aliquot of each individual sample was precisely transferred to an Eppendorf tube. After the addition of 185- μL pre-cooled (-40°C) extraction solution (acetonitrile/methanol/water, 80:80:25, with isotopically labeled internal standard), the sample was vortexed for 30 s and sonicated for 15 min in ice water bath. The solvent was then incubated at -40°C for 1 h and then centrifuged at 12,000 rpm at 4°C for 15 min. A 100- μL aliquot of the obtained supernatant was transferred to an auto-sampler vial for UHPLC-MS/MS analysis. Both acetonitrile and methanol were UPLC grade purchased from CNW Technologies (Shanghai Anpel Scientific Instrument Co., China).

UHPLC-MS/MS Analysis

The UHPLC separation was achieved using an Agilent 1290 Infinity II series UHPLC System (Agilent Technologies; Santa Clara, CA, USA), which was equipped with an ACQUITY UPLC BEH Amide column ($100 \times 2.1\text{ mm}$, $1.7\ \mu\text{m}$; Waters; Milford, MA, USA). The mobile phase A was 1% formic acid in water, while the mobile phase B was 1% formic acid in acetonitrile. The column temperature was set at 35°C . The auto-sampler temperature was at 4°C with an injection volume of 1 μL .

Further, an Agilent 6460 triple quadrupole mass spectrometer (Agilent Technologies; Santa Clara, CA, USA) was used, equipped with an electrospray ionization (AJS-ESI) interface (Agilent Technologies; Santa Clara, CA, USA). The ion source parameters were as follows: capillary voltage at $+4000/-3500\text{ V}$, nozzle voltage at $+500/-500\text{ V}$, gas (N_2) temperature at 300°C , gas (N_2) flow at 5 L/min, sheath gas (N_2) temperature at 250°C , sheath gas flow 11 L/min, and nebulizer pressure 45 psi.

Biomarker Analysis

All biomarker analyses were based on the R package *MetaAnalystR* 5.0. Use the random forest algorithm to sort by the contribution of features to the classification accuracy.

Both univariate and multivariate receiver operating characteristic (ROC) analyses were conducted. In the univariate analysis, the ROC curve was generated, with the area under the curve (AUC) and 95% confidence interval (CI) calculated. ROC curves and box plots of the five variables with the highest AUC were used. For multivariate ROC analysis, the model with the highest AUC was selected, and ROC curves based on the variables in this model were generated.

Statistical Analysis

All statistical analyses were performed using MetaboAnalyst 5.0 [22]. Every lipid feature was normalized according to the median intensity of each sample. Lipids with > 50% missing values were excluded, and the remaining missing values were replaced by the median intensity value for the lipid feature. Finally, log transformation and Pareto scaling were performed. A *t* test was performed using the Benjamini–Hochberg procedure to acquire the FDR and a paired *t* test was used to compare differences between groups. *P* values < 0.05 and FDR values < 0.25 were considered significant. Suspected outliers were excluded by a cautious investigation based on comprehensive interpretation using a heatmap, PCA, and outlier results by the random forest algorithm. PLS-DA models were cross-validated using leave-one-out cross-validation (LOOCV), and the *Q*₂ value was used to estimate overfitting of the model. Lipids with a VIP score value > 1 were defined as crucial for discriminating the groups. The Pearson correlation analysis was performed using the *rcorr* function in the *Hmisc* package 3.5.3 in R.

Results

Patient Demographic and Clinical Characteristics

After inclusion of all participants, we obtained their detailed clinical physiological and biochemical indicators. Comparisons between the two groups in sex (Fig. 1A), age (Fig. 1B), BMI (Fig. 1C), gallbladder function (Fig. 1D), hemoglobin (Fig. 1E), triglyceride concentration (Fig. 1F), glucose (Fig. 1G), cholesterol (Fig. 1H), and white blood cell count (Fig. 1I) are shown in Fig. 1. Except for gallbladder shrinkage rate, no significant differences were observed in other indicators between the stone group and control group.

Lipidome Profiling of Patients with Cholelithiasis

The PCA show that the sample composition 28 of patients with cholelithiasis group and 19 control groups is significantly separable. PC1 and PC2 have principal component scores of 51.1% and 10.2%, respectively (Fig. 2A).

The results show that the composition of samples in the group is consistent and the difference is small. It is obvious that regularity supports accuracy of the results. The results show that 123 lipids were significantly up-regulated and 43 lipids were significantly down-regulated (Fig. 2B). The results suggest that the change of LPC, FFA, and TAG are most pronounced (Fig. 2C). Therefore, the results show that FFA14:0, FFA16:1, LPC22:6 + Aco, and LPC14:0 + Aco increases significantly in the stone group (Fig. 2D).

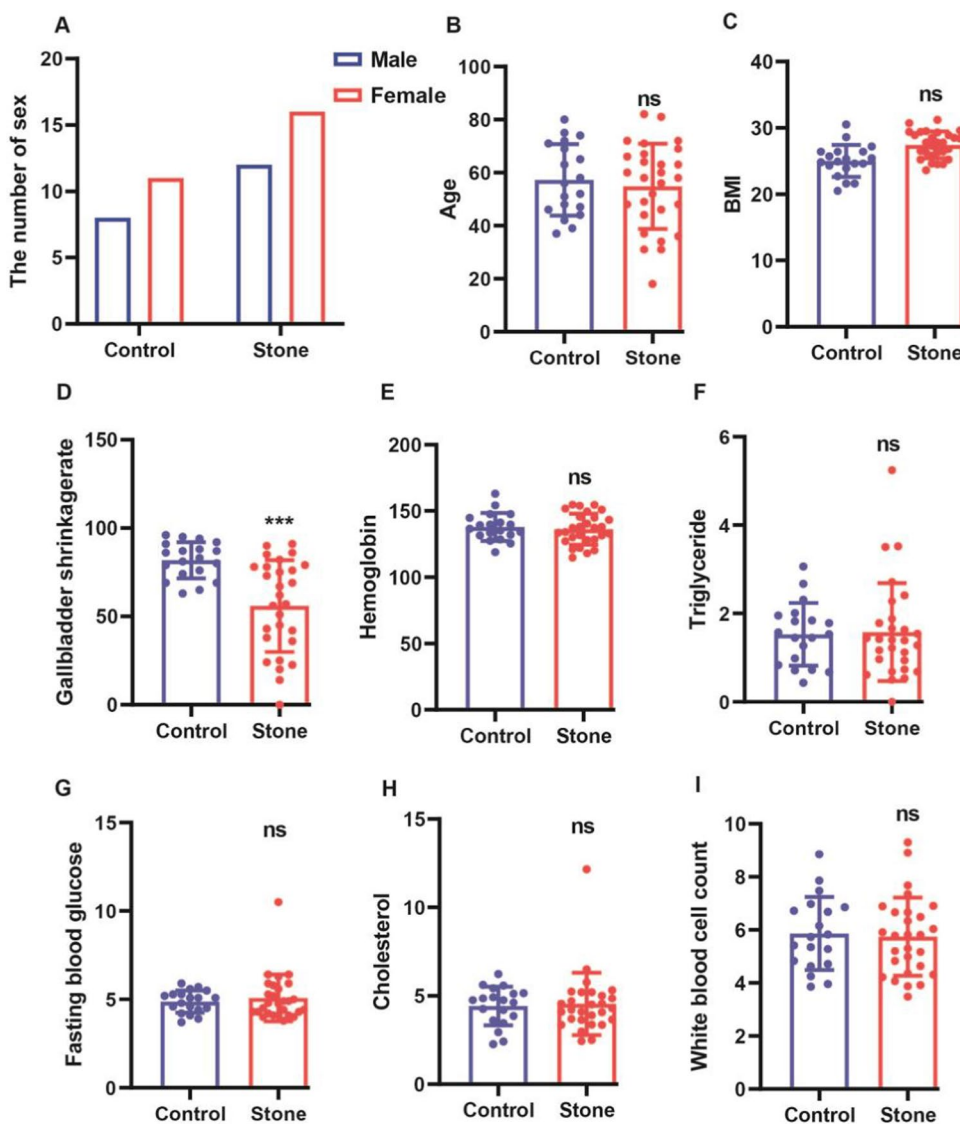
ROC of Lipidome Profiles in Patients with Cholelithiasis

We build a multivariate classification model with random forests. Six models were built using random forests. The six models separately were as follows: the number of metabolites is 5, AUC = 0.778, the number of metabolites is 10, AUC = 0.784, the number of metabolites is 15, AUC = 0.789, the number of metabolites is 25, AUC = 0.792, the number of metabolites is 50, AUC = 0.802, and the number of metabolites is 100, AUC = 0.806. Therefore, considering the number of variables and the power of the model, AUC is optimal when the number of metabolites is 15 (Fig. 3A). Next, for selection frequency, the higher its value, the more important the metabolite. Then, the analysis of selected frequency showed that LPC16:1 + Aco, PE-P 16:0–20:5, FFA 20:4, Hex2cer 18:1–16:0 and Hex2cer 18:1–24:1 were identified as the lipid species that could most effectively discriminate between the two groups (Fig. 3B). Therefore, the significant changes in FFA and LPC coincide with the previous results, once again verifying the reliability of the data. AUC-ROC curve show the area under the curve (AUC = 0.686). So, the results show that it distinguishes well between the stone group and the control group, and the sample data can be well distinguished (Fig. 3C). The figure shows accurate predictions: 24 accurate indicators are predicted in the disease model (Fig. 3D).

Prediction and Evaluation of Lipidome Profile Using Machine Learning Algorithms

To better verify the consistency of metabolite content trends and sample accuracy. We divide the samples into train set and test set. FFA.18.1 (Fig. 4A) and FFA.20.1 (Fig. 4B) of stone group were higher than control group in both train and test data sets. Similarly, LPC.16.0 (Fig. 4C) and LPC.20.1.Aco (Fig. 4D) of stone group were significantly higher than that of control group both in train set and test set. The above results indicate that the disorder of FFA.18.1, FFA.20.1, LPC16.0 and LPC20.1 were the main cause of cholelithiasis.

Fig. 1 Cholelithiasis population information. BMI (A), $P=0.3895$, age (B), $P=0.6419$, sex (C), gallbladder function (D), $P=0.0003$, hemoglobin (E), $P=0.6087$, triglyceride concentrations (F), $P=0.8762$, glucose (G), $P=0.5378$, cholesterol (H), $P=0.7919$, and white blood cell count (I), $P=0.7844$, ns, not significant



Analysis of Short-Chain Fatty Acid (SCFA) Profile of Patients with Choledocholithiasis

For SCFAs in the serum metabolome, Pearson correlation coefficient was applied to understand mutual regulatory relationships between SCFA metabolites [23]. The closer the absolute value of r was to 0, the weaker the degree between variables (Fig. 5A). The heatmap clustering algorithm grouped SCFAs into eleven blocks: the first block was constituted by isovaleric acid and the second by butyric acid (Fig. 5B). Here, the stone group vs control group is used as an example, and the results are shown in the figure below (Fig. 5C–F). The stone group had higher concentrations of butyric acid and isovaleric acid (Fig. 5C, D), but lower concentrations of octanoic acid and propionic acid than control group (Fig. 5E, F). Therefore, among the metabolites of the SCFA species, abnormalities in butyric acid, isovaleric acid,

octanoic acid, and propionic acid may be the main factor in the formation of choledocholithiasis.

ROC Analysis of SCFA in Serum From Stone and Control Group

Random forest was applied to identify SCFA species that could be used as biomarkers of choledocholithiasis. Six models were built using random forests. The six models separately were as follows: the number of metabolites is 2, $AUC=0.901$, the number of metabolites is 3, $AUC=0.95$, the number of metabolites is 5, $AUC=0.962$, the number of metabolites is 7, $AUC=0.959$, the number of metabolites is 10, $AUC=0.958$, and the number of metabolites is 11, $AUC=0.958$. Therefore, considering the number of variables and the power of the model, AUC is optimal when the number of metabolites is 10. The numbers of variables

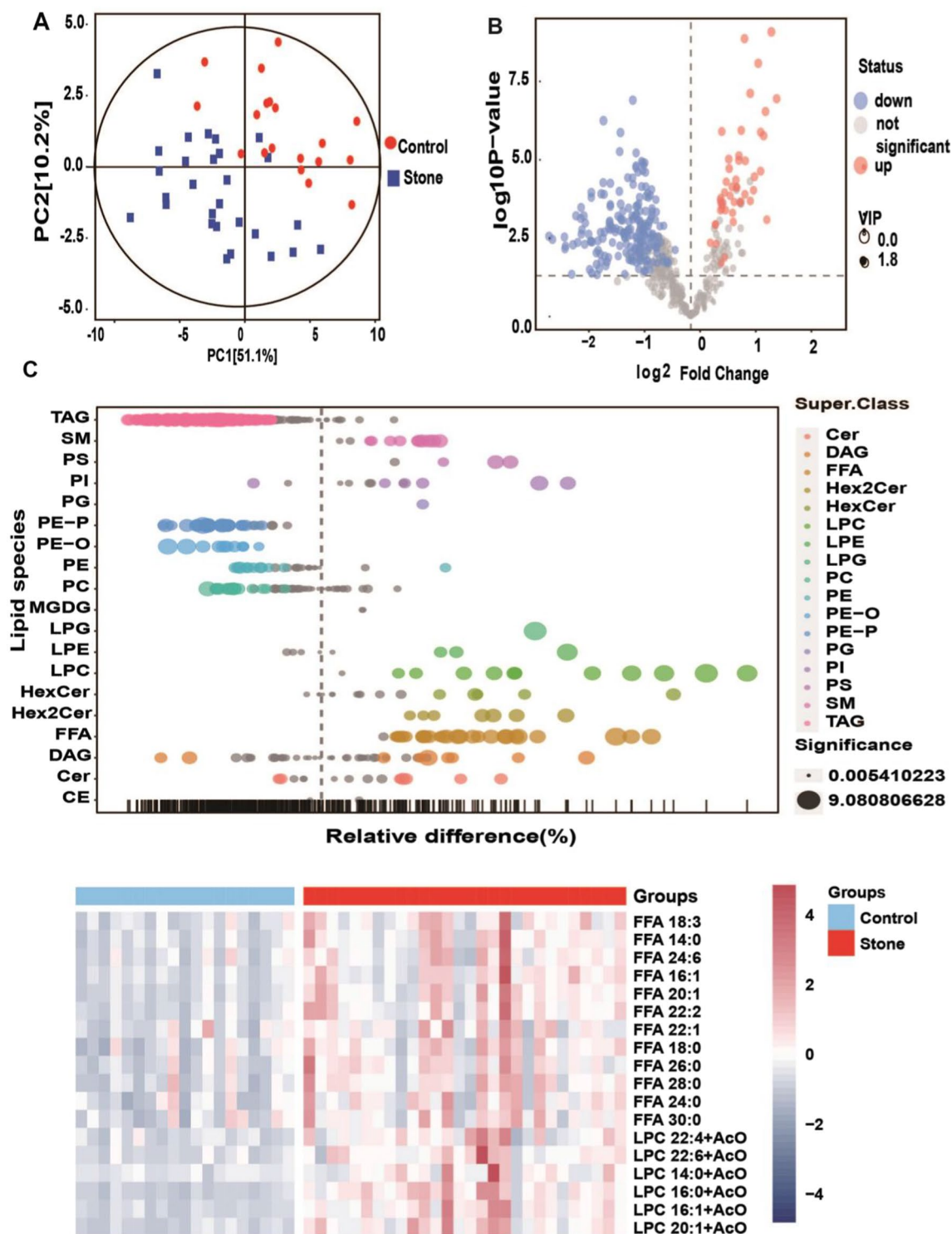


Fig. 2 The analysis of lipidome profile from cholecystolithiasis patients. PCA: Variable Importance in Projection (VIP) score identified FFA and LPC as the most effective lipids in distinguishing the groups of patients from the healthy volunteers. Score scatter plot of PCA model for group stone vs control (**A**). Differential metabolite screening volcano plot of the stone group versus the Control group.

Volcano plots identified the lipids species with the greatest changes were FFA and LPC (**B**). The lipid group bubble plot used the degree of change and difference in the content of metabolites (**C**). The heatmap clustering algorithm grouped the lipids into four blocks: The first three blocks were constituted mainly by oxylipins and the fourth by bile acids (**D**)

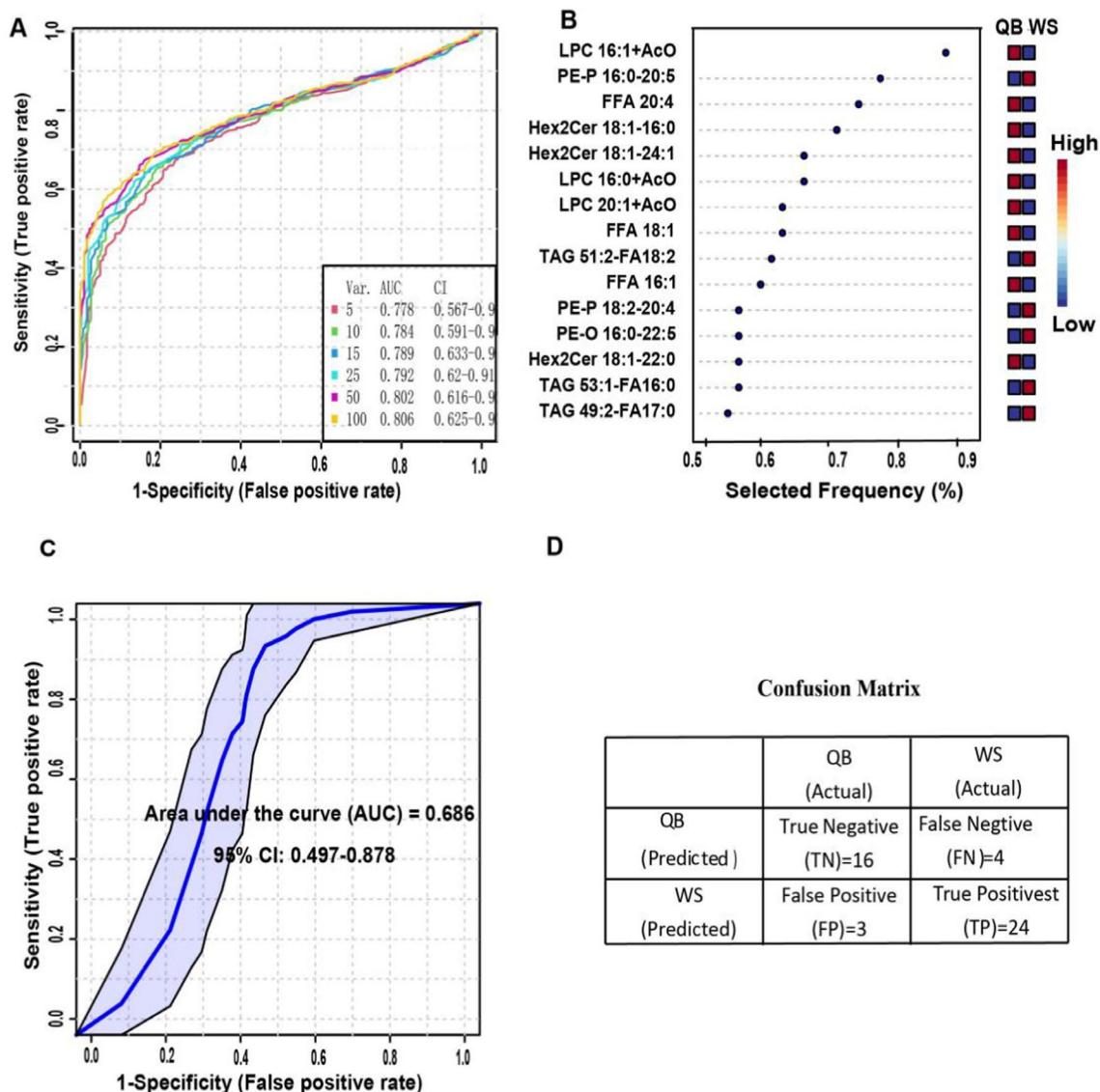


Fig. 3 ROC of Lipidome profiles in cholecystolithiasis patients. Receiver Operating Characteristics plot of random forest models corresponding to the combination of 5 to 100 variables (A). The most relevant parameters in the discrimination between both groups of patients were the FFA, LPC, and PE-P (B). The results showed that

differential expression of which was shown to be significant by the *t* test alone exhibited the best ROC curve for biomarker analysis (average under the curve AUC=0.686) (C). The figure shows accurate predictions: 24 accurate indicators are predicted in the disease model (D)

was progressively increased to 100 in 6 different models. In all instances, the analyses of the AUC-ROC curves were > 0.901 (Fig. 6A). The most relevant parameters in the discrimination between both groups were the butyric acid, propionic acid, isovaleric acid, and octanoic acid (Fig. 6B). The anastomosis of highly variable substances once again proves the reliability of the data. The results showed that the differential expression of which was shown to be significant by the *t* test alone exhibited the best ROC curve for biomarker analysis (average under the curve AUC=0.978) (Fig. 6C). The figure shows accurate predictions: 26 accurate indicators are predicted in the disease model (Fig. 6D).

The Analysis of Amino Acid Profile from Cholecystolithiasis Patients

The results show that the abscissa in the figure represents different experimental groups, the ordinate represents metabolites, and the color blocks at different locations represent the content of metabolites at the corresponding locations (Fig. 7A). 0.1-Methyl-L-histidine and 4-Hydroxyproline are lower in stone group than control group (Fig. 7B, C). On the contrary, glycine and L-Tyrosine are higher in stone group than control group (Fig. 7D, E).

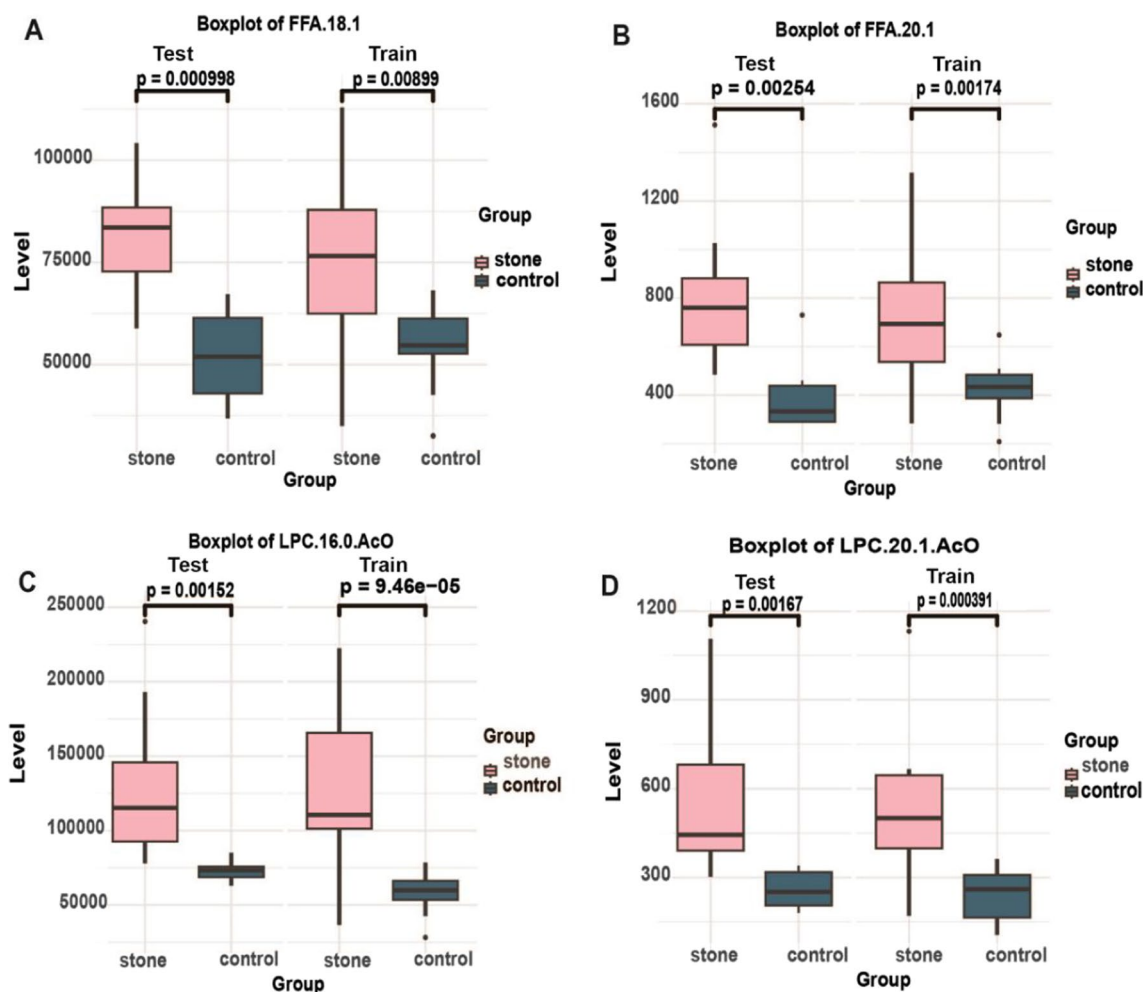


Fig. 4 The train and test analyses of lipidome profile from cholecystolithiasis patients. The data are generally divided into a test set and a training set for model learning prediction evaluation. FFA.18.1 (A) and FFA.20.1 (B) of cholecystolithiasis group were higher than con-

trol group both in train and test. Similarly, LPC.16.0.AcO (C) and LPC.20.1.AcO (D) of stone group were higher than control group both in train and test. The train and test analyses of lipid detected by the analysis are consistent with the above analysis. *** $P < 0.001$

ROC Analysis of Amino Acid in Serum from Stone and Control Group

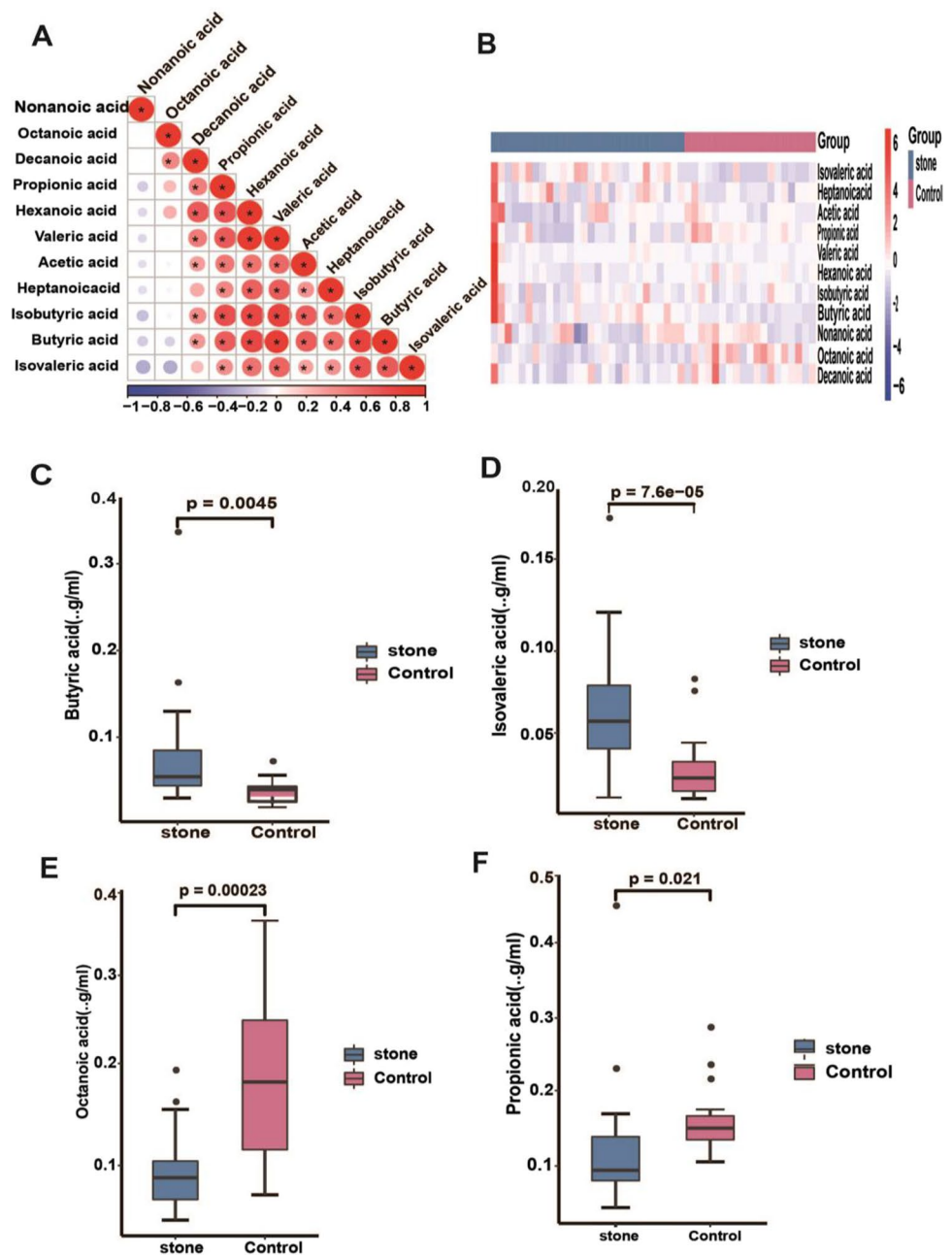
Six models were built using random forest. The six models separately were as follows: the number of metabolites is 2, AUC=0.994, the number of metabolites is 3, AUC=0.998, the number of metabolites is 5, AUC=1, the number of metabolites is 10, AUC=1, the number of metabolites is 20, AUC=1, and the number of metabolites is 25, AUC=1. Therefore, considering the number of variables and the power of the model, AUC is optimal when the number of metabolites is 15 (Fig. 8A). Receiver Operating Characteristics plot of Random Forest models corresponding to the combination of 2 to 25 variables (Fig. 8A). The most relevant parameters in the discrimination between both groups of patients were 1-Methyl-L-histidine and glycine (Fig. 8B). This result is consistent with the above results. The results

showed that the differential expression of which was shown to be significant by the *t* test alone exhibited the best AUC for biomarker analysis (average under the curve AUC=1) (Fig. 8C). The figure shows accurate predictions: 27 accurate indicators are predicted in the disease model (Fig. 8D).

Discussion

Cholecystolithiasis is a significant health problem, and 5% to 25% of the adult population are affected [3, 24]. The optimal treatment of cholecystolithiasis remains controversial [25]. Leukocytosis, liver function tests/bilirubin, and lactate should be paid with specific attention [26]. Accurate and rapid diagnosis of cholecystolithiasis remains a major clinical challenge. In this study, 28 consecutive patients scheduled for laparoscopic cholecystectomy for symptomatic

Fig. 5 The analysis of short acid profile from cholecystolithiasis patients. The closer the absolute value of *r* is to 1, the stronger the degree of association of the two variables, the closer *r* is to 0, and the degree of both variables weak (A). The heatmap clustering algorithm grouped the short acid into eleven blocks: The first blocks were constituted mainly by isovaleric acid and the second by butyric acids (B). Here, the stone group vs control group is used as an example, and the results are shown in the figure below (C–F). Butyric acid and isovaleric acid were higher in stone group than control group (C, D). Octanoic acid and propionic acid were lower in stone group than control group (E, F). **P* < 0.05, ***P* < 0.01, and ****P* < 0.001. *P* values were calculated using the two sample t test



cholecystolithiasis were included. The serum of these patients and volunteers was collected for multi-omics test. In this cross-sectional study, serum of multi-omics test analyzed to explore the metabolic characteristics of the microflora associated with cholecystolithiasis. Multi-omics test show that lipid, amino acids, and short-chain acid have a large difference between the gallstone group and the control group.

Lipids are essential metabolites that act as energy sources, membrane constituents, and signaling molecule [27]. Intrahepatic gallstones and pancreaticobiliary maljunction have a high risk for biliary malignancy. LPC is increased in the

bile of gallstone patients. It has reported that LPC-induced cytotoxicity causes senescence-associated secretory phenotype (SASP) in cholangiocytes [28]. In Pancreaticobiliary maljunction (PBM) and cholangiocarcinoma (CCA), LPC levels have been reported to be significantly elevated, together with increases in phospholipase A [29]. In addition, LPC also induce the production of cytotoxicity through the induction of apoptosis [30]. Furthermore, LPC causes the induction of senescence-associated secretory phenotype (SASP) to cellular senescence [31]. However, senescent cells can also play harmful effects on the tissue microenvironment. It is represented by the secretion of SASP and

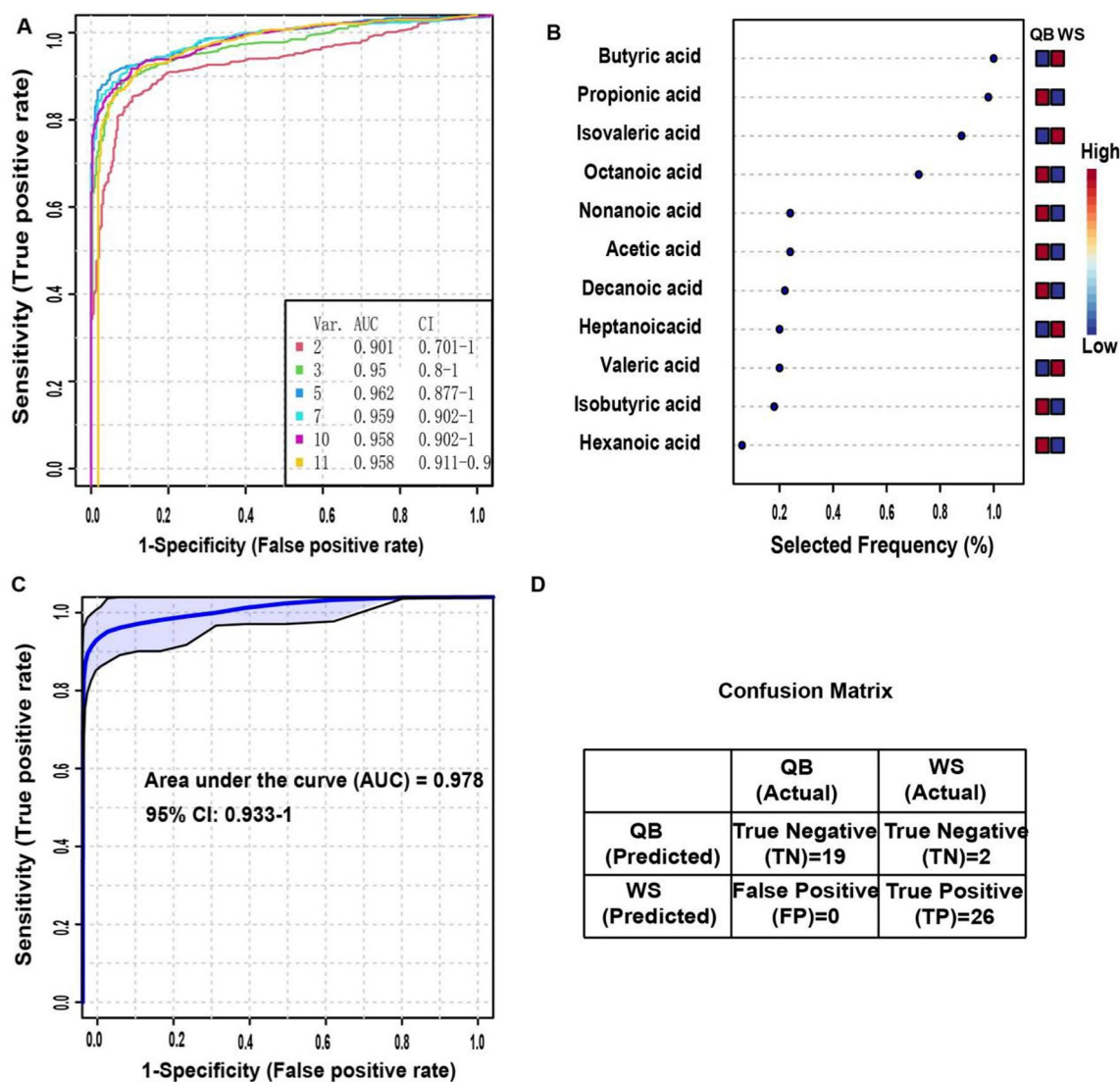


Fig. 6 ROC of short acid in serum from cholecystolithiasis and control group. Receiver Operating Characteristics plot of Monte Carlo models corresponding to the combination of 2–11 variables (A). The most relevant parameters in the discrimination between both groups of patients were the butyric acid, propionic acid, isovaleric acid, and

octanoic acid (B). The results showed that the differential expression of which was shown to be significant by the *t* test alone exhibited the best ROC curve for biomarker analysis (average under the curve AUC=0.978) (C). The figure shows accurate predictions: 26 accurate indicators are predicted in the disease model (D)

contributes to chronic inflammation and cancer progression [32]. As the results in this study show that LPC.16.0 and LPC.20.1 are significantly higher in stone group than in control group, it may suggest that the level of LPC in serum may be a reference indicator for clinical diagnosis.

In bile, the presence of FFA has been demonstrated [33, 34]. The elevated levels of bile FFAs were found to be an important and main risk factor for gallbladder wall thickening process [35]. FFAs are well-known risk factors of cardiovascular diseases (CVDs) [36] and have closely relationship with the events of metabolic syndromes (MetS), such as obesity and type 2 diabetes mellitus (T2DM). High levels of plasma FFAs are seen in obesity, because of more

FFAs by enlarged adipose tissue mass [37]. The increased level of FFAs in the bloodstream can impair endothelium-dependent vasodilation [38]. As the results in this study show that FFA.18.1 and FFA.20.1 are significantly higher in stone group than in control group, we speculate that FFAs in bile may play a role in promoting cholecystolithiasis. It may suggest that the level of FFAs in serum may be a reference indicator for clinical diagnosis.

However, patients with cholecystolithiasis have higher levels of branched chain amino acids (BCAAs) in serum that may be responsible for metabolic complications observed in these patients [39]. These studies suggest that amino acids may also play an important role in cholecystitis. In our study,

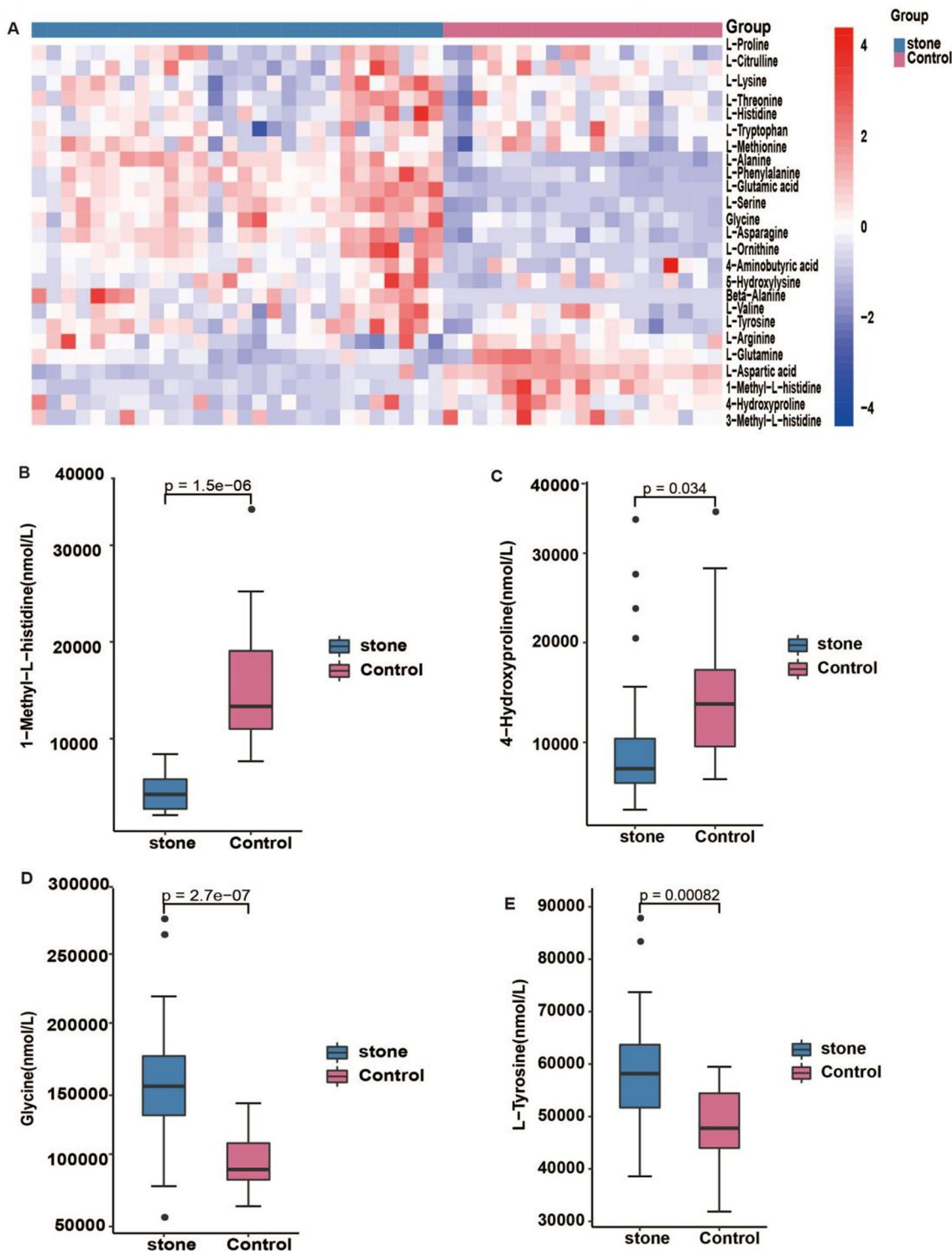


Fig. 7 The analysis of amino acid profile from cholecystolithiasis patients. Heatmap: The abscissa in the figure represents different experimental groups, the ordinate represents metabolites, and the color blocks at different locations represent the content of metabolites at the corresponding locations (A). For each group comparison, we calculated a significance *P* value for the quantitative value of

each metabolite, with different colors indicating different groupings of samples and using bins. Here, the stone group vs control group is used as an example, and the results are shown in the figure below (B–E). **P* < 0.05, ***P* < 0.01, and ****P* < 0.001. *P*-values were calculated using the two sample t test

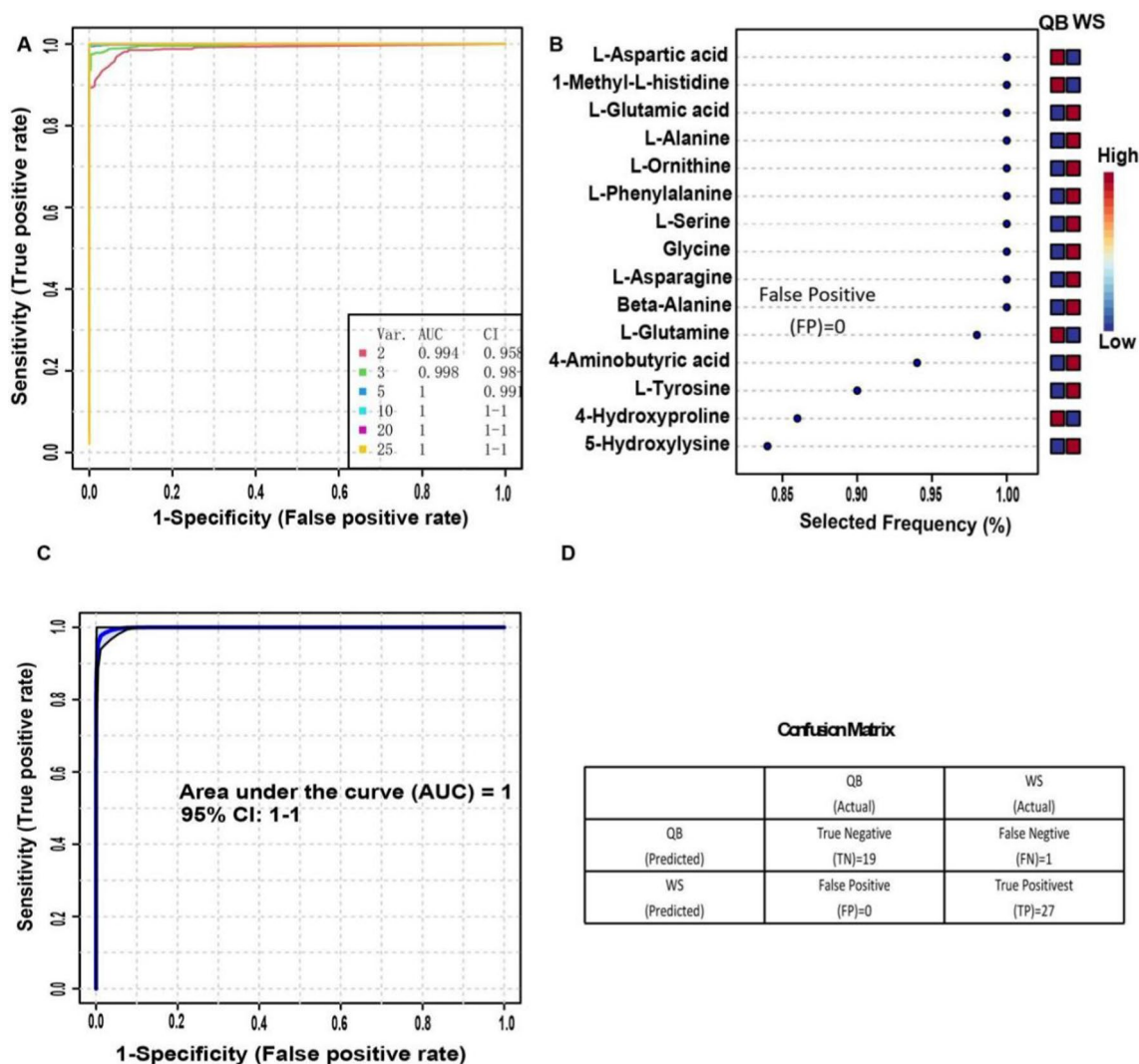


Fig. 8 The analysis ROC of amino acid in serum from cholecystolithiasis and control group. Receiver Operating Characteristics plot of Monte Carlo models corresponding to the combination of 2 to 25 variables (A). The most relevant parameters in the discrimination between both groups of patients were 1-Methyl-L-histidine and

glycine (B). The results showed that differential expression of which was shown to be significant by the *t* test alone exhibited the best ROC curve for biomarker analysis (average under the curve AUC=1) (C). The figure shows accurate predictions: 27 accurate indicators are predicted in the disease model (D)

results show that 1-Methyl-L-histidine and glycine play a vital role on cholecystolithiasis. Subsequently, BCAAs activate myocardial mammalian target of rapamycin signaling leading to cardiac dysfunction [40]. BCAAs likely promote insulin resistance by activating mammalian target of rapamycin complex [41]. The metabolism and accumulation of BCAAs changed in the blood may precede the development of insulin resistance and clinical manifestation of cardiometabolic diseases [42]. As the results in this study show that 1-Methyl-L-histidine and 4-Hydroxyproline are lower in stone group than control group. By the contrary, glycine and L-Tyrosine are higher in stone group than control group. It suggest that the level of BCAAs in serum may be a reference indicator for clinical diagnosis.

Free fatty acids (FFAs) are classified according to their aliphatic tail length; short-chain fatty acids (SCFAs) have fewer than 6 carbon atoms, medium-chain fatty acids (MCFAs) have 6–12 carbons, and long-chain fatty acids (LCFAs) have 12 or more carbons [43]. The anti-inflammatory function SCFAs are well known by modulating immune cell chemotaxis and reactive oxygen species (ROS) release [44]. SCFAs have been associated with anticancer activity on a variety of human cancer cell lines [44]. Studies have also reported that SCFAs were beneficial in colitis. When mice treated with butyrate had reduced inflammation in their colonic mucosa and reduced neutrophil infiltration [45]. SCFAs has been reported that it has relationship with the pathophysiology of several neurological disorders, such as

Alzheimer's disease, multiple sclerosis, Parkinson's disease, and amyotrophic lateral sclerosis [46]. The manipulation of SCFA levels in the intestinal tract of the microbiota structure can be potentially taken into consideration for cancer treatment/prevention [47]. Recently, studies have replayed that SCFAs can play a role on the progress of various diseases, such as inflammatory bowel disease (IBD), diabetes, atherosclerosis, and colorectal cancer (CRC) [48–50]. As the results in this study show that octanoic acid and propionic acid are lower in stone group than control group. By the contrary, butyric acid and isovaleric acid are higher in stone group than control group. It suggest that the level of SCFAs in serum may be a reference indicator for clinical diagnosis.

Therefore, there is great interest in identifying alternative and reliable biomarkers that can improve the assessment of treatment responses. This study aimed to investigate the serum biochemistry changes in gallstone patients and provide new clues for research on the involvement of gallstone formation. We found that patients with cholecystolithiasis had higher FFA and LPC than the healthy controls. This discovery will help develop new treatments for cholecystolithiasis and reduce the need for cholecystolithiasis surgery. Even restrictive resection strategies are not entirely ideal for patients with cholecystolithiasis and abdominal pain. Screening out cholecystolithiasis biomarkers is important to enable early detection and early treatment for cholecystolithiasis patients, thereby eliminating the need for surgery and reducing risk. The serum lipidomic profile associated with cholecystolithiasis is not well understood. Lipid metabolome analysis results showed that 542 lipids changed. Collectively, these results suggest that analysis of lipidome profiles is useful for identifying biomarker candidates that predict the evolution of preclinical to definitive cholecystolithiasis and could facilitate the assessment of disease activity and treatment outcomes. The analysis of SCFAs and amino acids profiles may be useful for identifying candidate biomarkers that predict progression of preclinical to clinically overt cholecystolithiasis, as well improving assessment of disease activity and treatment outcomes. This study not only discovered new targets for the clinical diagnosis and treatment of cholecystolithiasis but also opened a new door for cholecystolithiasis research.

Funding Funding was provided by the National Natural Science Foundation of China (12171285 and 11971269) and Program for Integrated Traditional Chinese and Western Medicine in Shandong Province of China (Grant Number YXH2019ZXY007).

Open Access This article is licensed under a Creative Commons Attribution-NonCommercial 4.0 International License, which permits any non-commercial use, sharing, adaptation, distribution and reproduction in any medium or format, as long as you give appropriate credit to the original author(s) and the source, provide a link to the Creative Commons licence, and indicate if changes were made. The images or other

third party material in this article are included in the article's Creative Commons licence, unless indicated otherwise in a credit line to the material. If material is not included in the article's Creative Commons licence and your intended use is not permitted by statutory regulation or exceeds the permitted use, you will need to obtain permission directly from the copyright holder. To view a copy of this licence, visit <http://creativecommons.org/licenses/by-nc/4.0/>.

References

1. Qiao T et al. Cholecystolithiasis is associated with *Clonorchis sinensis* infection. *PLoS One* 2012;7:e42471.
2. Einarrsson K et al. Influence of age on secretion of cholesterol and synthesis of bile acids by the liver. *N Engl J Med* 1985;313:277–282.
3. Kratzer W, Mason RA, Kächele V. Prevalence of gallstones in sonographic surveys worldwide. *J Clin Ultrasound* 1999;27:1–7.
4. Schirmer BD, Winters KL, Edlich RF. Cholelithiasis and cholecystitis. *J Long Term Eff Med Implants* 2005;15:329–338.
5. Shi JS et al. Studies on gallstone in China. *World J Gastroenterol* 2001;7:593–596.
6. Völzke H et al. Independent risk factors for gallstone formation in a region with high cholelithiasis prevalence. *Digestion* 2005;71:97–105.
7. Thunnissen FM et al. Healthcare utilisation of patients with cholecystolithiasis in primary care: a multipractice comparative analysis. *BMJ Open* 2021;11:e053188.
8. Pak M, Lindseth G. Risk Factors for Cholelithiasis. *Gastroenterol Nurs* 2016;39:297–309.
9. Kimura Y et al. Definitions, pathophysiology, and epidemiology of acute cholangitis and cholecystitis: Tokyo Guidelines. *J Hepatobiliary Pancreat Surg* 2007;14:15–26.
10. Gutt C, Schläfer S, Lammert F. The Treatment of Gallstone Disease. *Dtsch Arztebl Int* 2020;117:148–158.
11. Tazuma S et al. Nutritional factors (nutritional aspects) in biliary disorders: bile acid and lipid metabolism in gallstone diseases and pancreaticobiliary maljunction. *J Gastroenterol Hepatol* 2013;28:103–107.
12. Portincasa P, Moschetta A, Palasciano G. Cholesterol gallstone disease. *Lancet* 2006;368:230–239.
13. Jiang ZY et al. Increased expression of LXR alpha, ABCG5, ABCG8, and SR-BI in the liver from normolipidemic, nonobese Chinese gallstone patients. *J Lipid Res* 2008;49:464–472.
14. Wang, D.Q., D.E. Cohen, and M.C. Carey, *Biliary lipids and cholesterol gallstone disease*. *J Lipid Res*, 2009. **50 Suppl**: p. S406–11.
15. Wang HH et al. Effect of ezetimibe on the prevention and dissolution of cholesterol gallstones. *Gastroenterology* 2008;134:2101–2110.
16. Tazuma S. Homocysteine and gallstone diseases: is hyperhomocysteinemia a prerequisite for or secondary to gallstone formation? *J Gastroenterol* 2005;40:1085–1087.
17. Been JM, Bills PM, Lewis D. Microstructure of gallstones. *Gastroenterology* 1979;76:548–555.
18. Srivastava AK, Lal K, Tandon RK. A layerwise quantitation of human cholesterol gallstone constituents. *Indian J Med Res* 1983;77:733–738.
19. Maki, T., *Pathogenesis of calcium bilirubinate gallstone: role of E. coli, beta-glucuronidase and coagulation by inorganic ions, polyelectrolytes and agitation*. *Ann Surg*, 1966. **164**: p. 90–100.
20. Liu XT, Hu J. Relationship between bilirubin free radical and formation of pigment gallstone. *World J Gastroenterol* 2002;8:413–417.

21. Bugajska J et al. Characteristics of amino acid profiles and incretin hormones in patients with gallstone disease: a pilot study. *Pol Arch Intern Med* 2019;129:883–888.
22. Pang, Z., et al., *MetaboAnalyst 5.0: narrowing the gap between raw spectra and functional insights*. *Nucleic Acids Res*, 2021. **49**: p. W388-w396.
23. Adler, J. and I. Parmryd, *Quantifying colocalization by correlation: the Pearson correlation coefficient is superior to the Mander's overlap coefficient*. (1552–4930 (Electronic)).
24. McCain RS et al. Current practices and future prospects for the management of gallbladder polyps: A topical review. *World J Gastroenterol* 2018;24:2844–2852.
25. Guo T et al. Surgical methods of treatment for cholecystolithiasis combined with choledocholithiasis: six years' experience of a single institution. *Surg Endosc* 2022;36:4903–4911.
26. Kurzweil SM et al. Hyperbilirubinemia without common bile duct abnormalities and hyperamylasemia without pancreatitis in patients with gallbladder disease. *Arch Surg* 1994;129:829–833.
27. Han X. Lipidomics for studying metabolism. *Nat Rev Endocrinol* 2016;12:668–679.
28. Ohigashi T et al. Protective effect of phosphatidylcholine on lysophosphatidylcholine-induced cellular senescence in cholangiocyte. *J Hepatobiliary Pancreat Sci* 2019;26:568–577.
29. Sugiyama, Y., et al., *Altered bile composition in the gallbladder and common bile duct of patients with anomalous pancreaticobiliary ductal junction*. *World J Surg*, 2000. **24**: p. 17–20; discussion 21.
30. Fujita K et al. Partial characterization of proapoptotic action of biliary deteriorated lipids on biliary epithelial cells in pancreaticobiliary diseases. *J Hepatobiliary Pancreat Sci* 2014;21:212–218.
31. Shimizu R et al. Cholangiocyte senescence caused by lysophosphatidylcholine as a potential implication in carcinogenesis. *J Hepatobiliary Pancreat Sci* 2015;22:675–682.
32. Ohtani N, Hara E. Roles and mechanisms of cellular senescence in regulation of tissue homeostasis. *Cancer Sci* 2013;104:525–530.
33. Holloway RH, Heath T. Effect of oestradiol benzoate on biliary phospholipids in the rat. *Aust J Biol Sci* 1973;26:1009–1013.
34. Mingrone G, Greco AV, Passi S. The possible role of free fatty acids in the pathogenesis of cholesterol gallstones in man. *Biochim Biophys Acta* 1983;751:138–144.
35. Xiang Y et al. Free fatty acids and triglyceride change in the gallbladder bile of gallstone patients with pancreaticobiliary reflux. *Lipids Health Dis* 2021;20:97.
36. Egan BM, Greene EL, Goodfriend TL. Nonesterified fatty acids in blood pressure control and cardiovascular complications. *Curr Hypertens Rep* 2001;3:107–116.
37. Boden, G., *Obesity and free fatty acids*. *Endocrinol Metab Clin North Am*, 2008. **37**: p. 635–46, viii–ix.
38. Steinberg HO et al. Elevated circulating free fatty acid levels impair endothelium-dependent vasodilation. *J Clin Invest* 1997;100:1230–1239.
39. Behrendt A et al. VASOR: Accurate prediction of variant effects for amino acid substitutions in multidrug resistance protein 3. *Hepatol Commun* 2022;6:3098–3111.
40. Wang W et al. Defective branched chain amino acid catabolism contributes to cardiac dysfunction and remodeling following myocardial infarction. *Am J Physiol Heart Circ Physiol* 2016;311:H1160-h1169.
41. Bloomgarden Z. Diabetes and branched-chain amino acids: What is the link? *J Diabetes* 2018;10:350–352.
42. Tobias DK et al. Altered branched chain amino acid metabolism: toward a unifying cardiometabolic hypothesis. *Curr Opin Cardiol* 2018;33:558–564.
43. Kimura I et al. Free Fatty Acid Receptors in Health and Disease. *Physiol Rev* 2020;100:171–210.
44. Segain JP et al. Butyrate inhibits inflammatory responses through NFkappaB inhibition: implications for Crohn's disease. *Gut* 2000;47:397–403.
45. Vieira EL et al. Oral administration of sodium butyrate attenuates inflammation and mucosal lesion in experimental acute ulcerative colitis. *J Nutr Biochem* 2012;23:430–436.
46. Mirzaei R et al. Role of microbiota-derived short-chain fatty acids in nervous system disorders. *Biomed Pharmacother* 2021;139:111661.
47. Mirzaei R et al. Role of microbiota-derived short-chain fatty acids in cancer development and prevention. *Biomed Pharmacother* 2021;139:111619.
48. Kim CH. Microbiota or short-chain fatty acids: which regulates diabetes? *Cell Mol Immunol* 2018;15:88–91.
49. Ohira H, Tsutsui W, Fujioka Y. Are Short Chain Fatty Acids in Gut Microbiota Defensive Players for Inflammation and Atherosclerosis? *J Atheroscler Thromb* 2017;24:660–672.
50. Parada Venegas D et al. Short Chain Fatty Acids (SCFAs)-Mediated Gut Epithelial and Immune Regulation and Its Relevance for Inflammatory Bowel Diseases. *Front Immunol* 2019;10:277.

Publisher's Note Springer Nature remains neutral with regard to jurisdictional claims in published maps and institutional affiliations.

Authors and Affiliations

Kun Zhang^{1,2}  · Yongzheng Wang³ · Xiaoxuan Cui¹ · Wei Wang³ · Yuliang Li³

✉ Wei Wang
wwei0125@126.com

Kun Zhang
zhangkun@biotree.cn

Yongzheng Wang
wyzwxy911@sohu.com

Xiaoxuan Cui
cuixiaoxuan@biotree.cn

Yuliang Li
lyl.pro@sdu.edu.cn

¹ Shanghai Biotree Biotech Co. Ltd., Shanghai, China

² Institute of Basic Medical Sciences, The Second Hospital of Shandong University, Shandong 250033, China

³ Department of Interventional, The Second Hospital of Shandong University, Shandong 250033, China